



Physics at the LHC

Fabiola Gianotti

CERN, PH Department, 1211 Geneve 23, Geneve, Switzerland

editor: R. Petronzio

Available online 28 October 2004

Abstract

The CERN Large Hadron Collider (LHC) presents the most extraordinary challenges that particle physics has ever faced. By colliding high-intensity proton beams at a centre-of-mass energy of 14 TeV, it will unveil the previously unexplored territory of the TeV scale in great detail. We survey the fundamental physics questions which the LHC is expected to address, and illustrate the physics potential with several examples from a very broad programme. Comparisons with results from current experiments and with the potential of future machines are also made for some key cases.

© 2004 Elsevier B.V. All rights reserved.

PACS: 10.

Keywords: LHC; Challenges; Discoveries

1. Introduction

Although the Standard Model (SM) has been verified with spectacular accuracy, i.e. to 0.1% or better in most cases [1], by experiments performed at various machines (e.g. at the CERN LEP collider), there are numerous indications today that the SM is not the ultimate theory of elementary particles and their interactions. They include, among others, the recent evidence for atmospheric [2] and solar [3] neutrino oscillations, and the incapacity of the SM to give satisfactory answers to fundamental questions [4] such as the mass and flavour problems, baryogenesis and the matter–antimatter asymmetry in the universe, the origin of dark matter, the size of the cosmological constant, and the unification of gravity with the other interactions.

E-mail address: fabiola.gianotti@cern.ch (F. Gianotti).

The most urgent issue is to explain the origin of the particle masses. The SM Higgs mechanism has received no experimental confirmation as yet, and the lower limit on the mass of the Higgs boson ($m_H > 114.4$ GeV from direct searches at LEP [5]) has become close to the indirect upper bound derived from a fit to the electroweak data ($m_H < 251$ GeV at the 95% C.L. [1]), which starts to raise questions about the internal consistency of the theory. Furthermore, in the SM the mass of the Higgs boson, which is the only scalar of the theory, increases, through radiative corrections, with the energy scale Λ up to which the SM is valid, and therefore requires a large amount of “fine tuning” to be stabilized at the electroweak scale (the so-called “naturalness” problem). Finally, the generation of fermion masses spoils the simplicity of the theory with a proliferation of unknown (and apparently random) parameters.

The above arguments open the door to new and more fundamental physics [4]. There are today several candidate scenarios for physics beyond the Standard Model, including Supersymmetry (SUSY), Technicolour and theories with Extra-dimensions. All of them predict new particles in the TeV region, as needed to stabilize the Higgs mass. We note that there is no other scale in particle physics today as compelling as the TeV scale, which strongly motivates a machine like the LHC able to explore directly and in detail this energy range.

We discuss in this paper the capability of the LHC experiments, ALICE [6], ATLAS [7], CMS [8] and LHCb [9], to address and hopefully resolve some of the above questions. After a brief introduction on the main features of pp interactions at 14 TeV (Section 2), we present examples of the very broad LHC physics potential: precise measurements of CP-violation (Section 3), searches for the SM Higgs boson (Section 4), searches for Supersymmetry and other scenarios beyond the Standard Model (Section 5), studies of quark–gluon plasma in ultra-relativistic heavy-ion collisions (Section 6).

The LHC detectors, their performance and the main experimental challenges (e.g the event pile-up at high luminosity) are described in [10], while the machine is discussed in [11].

The LHC is a 30-year project. First discussions took place in a historical workshop held in Lausanne in 1984 [12], and were followed by a vigorous detector R&D activity focussing in particular on radiation-hard and fast-response technologies. The experiment construction started in mid 1990s, while operation will begin in 2007 and last more than 10 years. Since 1984, our understanding of particle physics has evolved significantly, driven by the extremely precise and detailed electroweak measurements from LEP and SLC, and the discovery and measurement of the top quark at the Tevatron. The high-energy operation of LEP2 pushed the mass limit on the Higgs boson far beyond the most optimistic expectations. All of these extraordinary results have served to confirm the Standard Model in detail, while the need for physics beyond it has become more apparent. Thus, the motivation for the LHC, and its expected physics potential, have only become stronger and stronger with time.

2. Physics at the LHC: main assets and main challenges

Operation at a high-energy and high-luminosity hadron collider like the LHC brings many advantages and some difficulties. The main advantage is that the event rate will be huge, so that the LHC will become a factory of all particles with masses up to a few TeV which have reasonable couplings to SM particles. This is illustrated in Table 1 which shows, for some representative processes both from known and new physics, the expected event production rates in ATLAS and CMS in the first years of operation, when the machine luminosity will be about a factor of 10 lower than the design luminosity $L = 10^{34}$ cm⁻² s⁻¹. Even in these more conservative conditions, and taking into account detection efficiencies, millions of

Table 1

Process	Evts/s	Evts/year	Total samples from previous colliders
$W \rightarrow e\nu$	15	10^8	10^4 events LEP, $\sim 10^6$ events Tevatron
$Z \rightarrow ee$	1.5	10^7	10^6 events LEP
$t\bar{t}$	1	10^7	$\sim 10^4$ events Tevatron
$b\bar{b}$ (LHCb)	10^5	10^{12}	$\sim 10^9$ events BaBar, Belle
$\tilde{g}\tilde{g} \ m = 1 \text{ TeV}$	10^{-3}	10^4	—
$H \rightarrow \gamma\gamma \ m_H = 120 \text{ GeV}$	10^{-5}	~ 130	—

For the physics channels listed in the first column, the expected numbers of events produced in each experiment per second (second column) and over 1 year of data taking (third column). All numbers correspond to the initial low luminosity of $L = 10^{33} \text{ cm}^{-2} \text{ s}^{-1}$ foreseen in ATLAS and CMS, except for the $b\bar{b}$ process, for which $L = 2 \times 10^{32} \text{ cm}^{-2} \text{ s}^{-1}$, as required by the LHCb experiment, has been assumed. The total event samples collected (or expected to be collected) at colliders operating before the LHC start-up are given in the last column.

events should be collected for many SM channels over only 1 year of data taking, yielding samples much larger than those accumulated by previous colliders over their whole life time. Hence, thanks to a seven-fold increase in energy and a ten-fold increase in luminosity compared to the Tevatron, the LHC will immediately enter new territory as soon as it turns on. Major discoveries could very well follow during the first year of operation. With more luminosity and time, the mass for the direct discovery of new heavy particles should be ultimately pushed up to masses of $\sim 5\text{--}6 \text{ TeV}$.

At the same time, both the high energy and high luminosity entail several experimental challenges, which set stringent requirements on the trigger and detector performance. The main difficulty related to the high centre-of-mass energy is illustrated in Fig. 1, which shows the production cross-sections for several channels at hadron colliders, as a function of \sqrt{s} . One can notice two features. First at the LHC, just as in previous hadron colliders, the high- p_T event rate will be dominated by QCD jet production, a strong process with a huge cross-section. In contrast, the most interesting physics channels are usually much rarer either because they involve the production of heavy particles, or because they arise from electroweak processes (e.g. W or Higgs production). It can be seen for example that at 14 TeV the cross-section for jets with $p_T > 100 \text{ GeV}$ is five orders of magnitude larger than the cross-section for a Higgs boson of mass 150 GeV. As a consequence, in contrast to e^+e^- machines, there is no hope for experiments at the LHC to detect a Higgs boson decaying into jets, unless it is produced in association with other particles giving a cleaner signature (see Section 4), since such final states will be swamped by the much larger QCD background. Decays into leptons or photons have to be used instead, so that in general only part of the available cross-section is de facto usable. Similar arguments apply to any other relatively light (mass in the few hundred GeV range) object, whereas the situation improves for very massive particles (e.g. an excited quark in the TeV range decaying as $q^* \rightarrow qg$) since the QCD background decreases fast with the invariant mass of the final-state products. In addition, because the probability for a jet to fake an electron or photon is small but non-vanishing, and because of the huge differences between the signal and background cross-sections for many interesting processes, excellent detector (and trigger) performance in terms of particle identification capability and energy resolution are needed in order to extract a clean signal above the various reducible and irreducible backgrounds. For example, mass resolutions of $\sim 1\%$ for objects decaying into leptons or photons, and rejection factors against jets faking photons larger than 10^3 , are required.

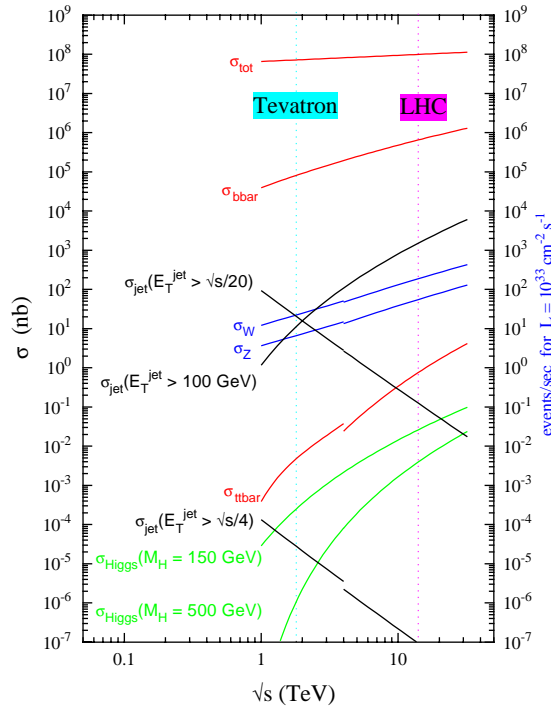


Fig. 1. Production cross-sections for various processes at hadron colliders (pp and $p\bar{p}$), as a function of the machine centre-of-mass energy. The discontinuities in some of the curves are due to the transition from $p\bar{p}$ to pp collisions.

The second aspect to notice is that QCD cross-sections grow much faster with \sqrt{s} than electroweak cross-sections. For instance, the W and Z cross-sections are a factor of 10 higher at the LHC energy than at the Tevatron energy, whereas $t\bar{t}$ production (a strong process) is a factor of 100 larger. This is due to the strongly enhanced gluon component in the proton parton density distributions at the LHC energies (the LHC is essentially a gluon–gluon collider). As a consequence, although signal rates will be larger at the LHC than at the Tevatron, signal-to-background ratios are expected to be worse in many cases.

The main difficulty related to operating at $L = 10^{34} \text{ cm}^{-2} \text{ s}^{-1}$, which will be a factor of about 100 higher than the instantaneous luminosity achieved so far at the Tevatron, is that the interaction rate will be 10^9 Hz . Hence, at each bunch crossing, i.e. every 25 ns, an average of about 20 low- p_T events (so-called “minimum-bias”) will be produced simultaneously in the ATLAS and CMS detectors. The impact of this event “pile-up” on the design of the LHC detectors in terms of response time, radiation hardness and granularity, as well as on their performance, is discussed in [10]. From the physics point of view, the pile-up has an impact mainly on the calorimeter mass resolution for light particles, on the missing transverse energy resolution, and on the effectiveness of some tools (e.g. jet veto and forward jet tag) used to extract possible signals from the background.

Finally, it should be noted that fast and highly selective trigger systems are needed, with the ability to reduce the initial event rate of 10^9 Hz to a rate-to-storage of $\sim 100 \text{ Hz}$ while preserving high efficiency for the interesting physics processes. This is also discussed in [10].

3. Precise measurements of CP-violation

One of the main lessons from the Tevatron experiments is that precision physics is possible at hadron colliders. In this respect the LHC experiments will benefit from two advantages compared to CDF and D0: more powerful and higher-performance detectors, and much larger event samples. They should therefore be able to make several precise measurements of SM particles and processes, in particular in the case of ATLAS and CMS during the initial phase at $L \leq 10^{33} \text{ cm}^{-2} \text{ s}^{-1}$ when the experimental environment will be very similar to that at the Tevatron. These measurements represent a complementary approach to direct searches for new particles, being also sensitive to new physics but in an indirect way, i.e. through loop corrections to the measured observables. Here we only discuss one example, namely the measurement of CP-violation by the LHCb experiment. A complete overview of precision physics at the LHC can be found in Ref. [13].

CP-violation is one of the outstanding questions in particle physics. It was first discovered [14] and established in the kaon system, for which the most precise measurement today comes from the CERN NA48 experiment [15]: $Re(\epsilon'/\epsilon) = (14.7 \pm 2.2) \cdot 10^{-4}$.

The LEP experiments [16] and CDF have performed many studies of the B -system, but only in the year 2001, with the advent of the SLAC and KEK B-factories, the first significant observation of CP-violation in B -decays has been obtained. The BaBar [17] and Belle [18] experiments, operating at the PEP II/SLAC and KEKB/KEK e^+e^- machines, respectively, have unambiguously established the non-vanishing value of $\sin 2\beta$, one of the angles of the CKM unitarity triangle (present world average: $\sin 2\beta = 0.736 \pm 0.049$).

The most intriguing issue in this field, relevant to both particle physics and cosmology, is that the above experimental measurements confirm, within their uncertainties, the (tiny) CP-violation predicted by the Standard Model, which is a consequence of the quark mass generation and of a phase in the quark-mixing CKM matrix. The problem is that this amount of CP-violation is insufficient to explain baryogenesis and the ensuing matter–antimatter asymmetry in the universe, which calls for additional contributions from new physics. The task of present and future B -physics experiments is therefore to clarify this puzzle, by performing precise, comprehensive, and redundant studies of CP-violating effects in the B -system, which should test the internal coherence of the Standard Model (and disclose possible inconsistencies), shed some light on the origin of CP-violation, and probe the existence of new physics.

Fig. 2 shows the triangle obtained from the unitarity constraints of the CKM matrix. The sides of this triangle can be determined by measuring B -decay branching ratios and B -mixing, whereas the angles α, β, γ are related to CP-violating decays of B -mesons, and can therefore be inferred from the observed time-dependent asymmetries in the rates of final-state products. In principle, once the sides of the triangle are determined, the angles are also constrained. However, it is of utmost importance to compare these indirect determinations with direct measurements of α, β, γ , in order to perform stringent tests of the internal consistency of the theory.

Prior to 2007, BaBar, Belle, CDF and D0 will provide several measurements of the unitarity triangle: $\sin 2\beta$ will likely be known to better than 0.02 from the $B_d^0 \rightarrow J/\psi K_S^0$ decay asymmetry; the sides $|V_{ub}|/|V_{cb}|$ and $|V_{td}|/|V_{cb}|$ may be determined to 5–10% (dominated by the theoretical uncertainty) from $b \rightarrow u, c$ transitions and $B^0 - \bar{B}^0$ mixing; the precision on the angle α will probably be ~ 0.1 , limited by statistics and theoretical uncertainties; the angle γ will be largely unconstrained. These and other measurements will provide a lot of information to construct the triangle. However, because of the limited statistics in some cases and the lack of sensitivity of the present experiments to some channels, they will

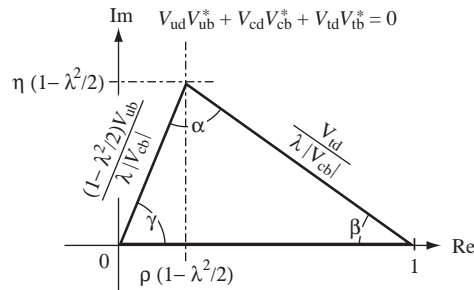


Fig. 2. One of the unitarity triangles derived from the parameters and constraints of the CKM matrix, in the Wolfenstein parametrization.

not allow the theory to be over-constrained, and therefore may not reveal inconsistencies of the Standard Model even in the presence of new physics. B -physics measurements beyond those achievable at today's machines are therefore motivated by the need of improving the study of CP-violation up to the level where the Standard Model can be uncontroversially and redundantly tested, and possible evidence for new physics can be extracted. These studies must include the B_s^0 system, which is not accessible at the present B-factories running at the $\Upsilon(4s)$, and which will provide additional crucial information, as detailed below. Furthermore, B -meson decays involving loops, in particular rare decays strongly suppressed in the Standard Model (e.g. $B \rightarrow \mu\mu$), are a clean laboratory to look indirectly for new physics contributing new particles to such loops.

The above goals require high-statistics samples of the various B -meson species, which can only be collected at hadron machines. Historically these machines have played an important rôle, since beauty was discovered in hadronic collisions, the first evidence for mixing came from the UA1 experiment, and the Tevatron has provided first studies of the B_s mesons.

The LHC will be the most copious source of b -quarks ever (see Table 1), yielding samples of more than 10^{12} events/year, consisting of a mixture of 40% of B_u , 40% of B_d , 10% of B_s , and 10% of B_c and B -baryons. The dedicated LHCb experiment [9,10] has been designed to exploit fully these data, with five main features: it will run at a luminosity of $2 \times 10^{32} \text{ cm}^{-2} \text{ s}^{-1}$ in order to avoid multiple interactions in the same bunch-crossing and to limit the radiation damage; it has a powerful trigger, using also the vertex-detector information, able to select not only final states containing leptons, but also fully hadronic events (this is challenging since less than 1% of all inelastic collisions produce b -quarks); it includes two RICH detectors in order to separate kaons from pions over the momentum range 2–100 GeV, which is crucial in particular to study B_s mesons; it has high-resolution and redundant vertex detectors, expected to provide powerful tagging of secondary vertices, precise measurements of time-dependent asymmetries (with a proper-time resolution of ~ 35 fs), and the capability of resolving rapidly oscillating systems like B_s mesons; it can achieve an excellent B -mass resolution of typically ~ 12 MeV, which will offer additional handles against the various backgrounds.

LHCb will perform a large variety of precise measurements in the B -system, and in particular it will be able to measure all three angles of the unitarity triangle [9,13]. ATLAS and CMS will also participate in this programme, contributing significantly to the measurement of $\sin 2\beta$ to ~ 0.01 during the initial phase at low luminosity, and to the study of rare $B \rightarrow \mu\mu$ decays. However, the distinctive and unique asset of LHCb, compared to present machines and to ATLAS and CMS, is the possibility to measure the angle γ , and to disentangle the Standard Model contribution from possible sources of new physics. The angle γ can

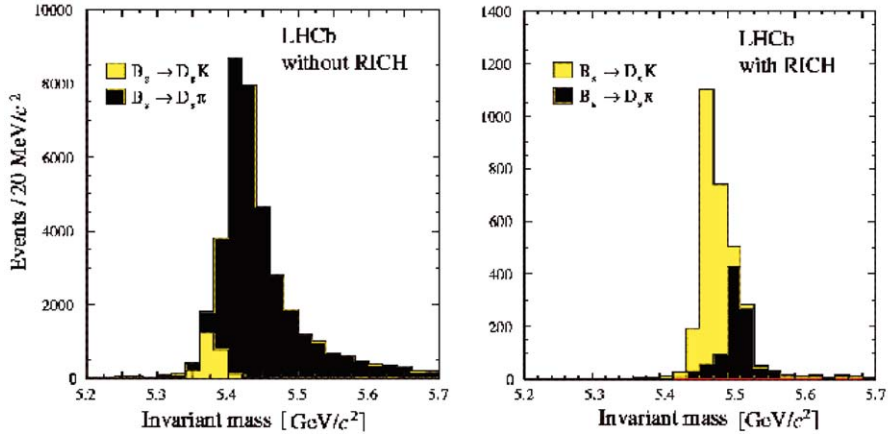


Fig. 3. The reconstructed $B_s \rightarrow D_s K$ mass spectrum (gray histogram) on top of the $B_s \rightarrow D_s \pi$ background (black histogram), obtained from a simulation of the LHCb experiment without (left panel) and with (right panel) the information of the RICH detectors.

be obtained from the time-dependent decay rates of a combination of channels, including $B_s^0 \rightarrow D_s^\mp K^\pm$, $B_d^0 \rightarrow \pi^+ \pi^-$, $B_s^0 \rightarrow K^+ K^-$, $B_d^0 \rightarrow D^{*\pm} \pi^\mp$, etc. Most of these processes are not accessible at present B-factories and at the Tevatron, nor to ATLAS and CMS mainly because of their modest K/π separation capabilities. In contrast, Fig. 3 shows the clean $B_s \rightarrow D_s K$ mass peak expected in LHCb if the particle identification power of the RICH detectors is used. The interest of the above channels is that they are characterized by different types of decay diagrams: tree decays, or decays occurring through loops (so-called “penguin”), or diagrams containing flavour-mixing boxes. In the absence of new physics, all the above measurements should give the same value of γ , i.e. $\gamma \approx 65^\circ$, which is the preferred value in the Standard Model. If new physics is there, it will in general contribute to penguin diagrams and/or box diagrams, whereas the tree-diagrams will not be “polluted”. Therefore different values of γ will be obtained from the measurements of the various processes. A combined comparative analysis of all channels should therefore provide a clean determination of the CKM parameters regardless of new particles in virtual loops, and at the same time possible evidence for CP-violation beyond the Standard Model predictions, together with useful indications to identify the corresponding underlying physics scenario.

4. Searches for the SM Higgs boson

Today, after more than 10 years of searches and a wealth of beautiful precision measurements performed mainly at CERN (LEP), our knowledge about the SM Higgs boson can be summarized as follows. Its mass is not specified by the theory, which provides only an upper bound of ~ 1 TeV. Direct searches performed at LEP have set a lower limit of $m_H > 114.4$ GeV [5]. In the year 2000, the last year of LEP operation, a few events with features compatible with those expected from the production of a Higgs boson of mass ~ 115 GeV have been observed, but the size of the effect is too small to claim a discovery [19]. Finally, a fit of the Standard Model to the ensemble of data collected by various machines (LEP, Tevatron, SLC) gives a 95% C.L. upper bound on m_H of about 250 GeV [1]. The current experimental data therefore favour a light Higgs boson.

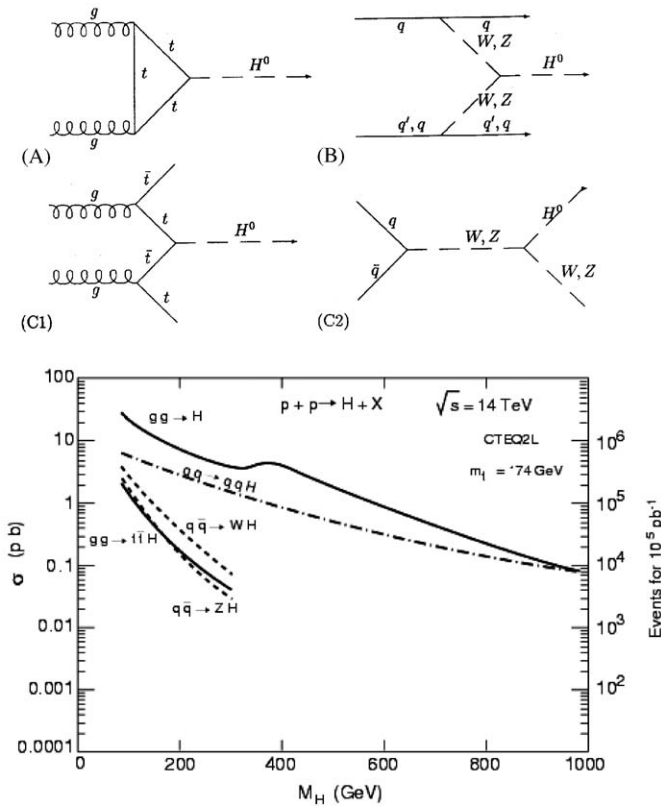


Fig. 4. Top panel: main Feynman diagrams contributing to the production of a SM Higgs boson at the LHC: (A) gg -fusion, (B) WW and ZZ fusion, (C1) associated $t\bar{t}H$ production, (C2) associated WH and ZH production. Bottom panel: expected production cross-sections for a SM Higgs boson at the LHC as a function of mass.

In contrast to its mass, the Higgs decay modes are known, because the SM predicts that this particle couples to fermions and bosons with strength proportional to their masses. Therefore, for $m_H < 120 \text{ GeV}$ the Higgs boson should decay mainly into $b\bar{b}$, whereas for larger masses decays into W pairs and Z pairs should dominate.

The production of a Standard Model Higgs at the LHC is expected to proceed mainly through the diagrams shown in Fig. 4. The cross-sections for these processes are shown in the same figure as a function of mass. Gluon–gluon fusion through a top-quark loop is the dominant production channel for all masses. Vector boson (WW , ZZ) fusion contributes about 20% of the cross-section for $m_H \sim 120 \text{ GeV}$ and becomes more and more important with increasing mass. This process leads to the very distinctive topology of a Higgs boson accompanied by two jets emitted in the forward regions of the detector and very little activity in the central region (since no colour lines are exchanged between the two interacting bosons). Higgs production with a $t\bar{t}$ pair or a W/Z boson has a smaller cross-section; however it allows detection of the purely hadronic $H \rightarrow b\bar{b}$ decay mode, because the reconstruction of the particles produced in association with the Higgs provides additional handles against the large QCD backgrounds.

The resulting LHC discovery potential for one experiment is summarized in Fig. 5 (ATLAS is shown here but CMS has a similar reach). One can notice several features. First, a SM Higgs boson can be

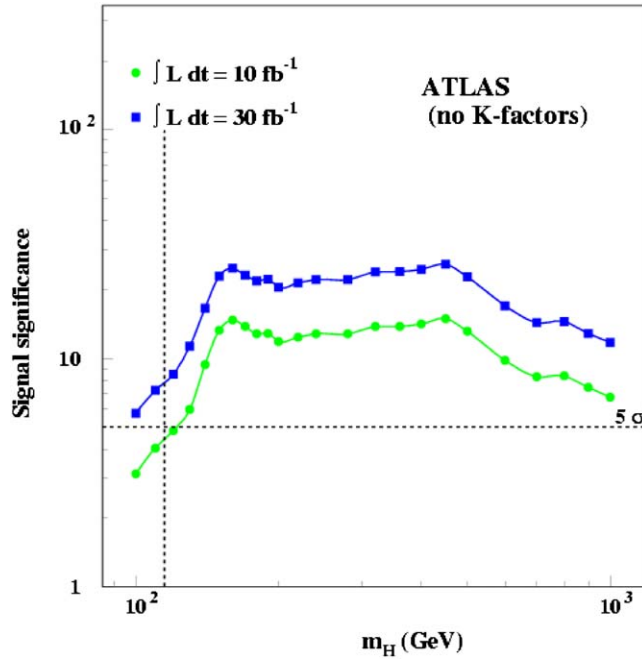


Fig. 5. The expected signal significance for the discovery of a SM Higgs boson in ATLAS as a function of mass, for integrated luminosities of 10 fb^{-1} (dots) and 30 fb^{-1} (squares). The vertical line shows the mass lower limit from LEP. The horizontal line indicates the minimum significance (5σ) needed for discovery.

discovered over the full allowed mass range ($114.4 \text{ GeV} - 1 \text{ TeV}$) with only 10 fb^{-1} of integrated luminosity, which corresponds (in principle) to only 1 year of LHC operation at low luminosity. In practice, more time will be needed at the beginning to understand and calibrate complex detectors like ATLAS and CMS, and to measure and control the backgrounds at the required level, so that extracting a convincing signal will most likely take more than one year.

Second, Higgs boson discovery should be easier and faster for masses above 200 GeV , thanks to the “gold-plated” $H \rightarrow ZZ \rightarrow 4\ell$ (where $\ell = e, \mu$) channel, which is essentially background-free. In contrast, the most difficult region is the best motivated low-mass region close to the LEP limit and at the overlap with the Tevatron reach.¹ The expected sensitivity for $m_H = 115 \text{ GeV}$ and for the first good 10 fb^{-1} is detailed in Table 2. The total significance of about 4σ per experiment ($4_{-1.3}^{+2.2} \sigma$ including the expected systematic uncertainties) is more or less equally shared among three channels (see also Fig. 6): $H \rightarrow \gamma\gamma$, $t\bar{t}H$ production with $H \rightarrow b\bar{b}$, and Higgs production in vector-boson fusion followed by $H \rightarrow \tau\tau$.

A conservative approach has been adopted in deriving these results. For instance, very simple cut-based analyses have been used, and higher-order corrections to the Higgs production cross-sections (the so-called K-factors), which are expected to increase for example the $gg \rightarrow H \rightarrow \gamma\gamma$ rate by a factor of ~ 2 compared to leading order, have not been included. Nevertheless, it will not be easy to extract

¹ The present estimate of the Tevatron reach by the year 2009 (expected integrated luminosity $\sim 8 \text{ fb}^{-1}$) can be summarized as follows [20]: a 95% C.L. exclusion could be achieved up to masses of about 135 GeV and a 5σ observation up to masses of 115 GeV .

Table 2

For a Higgs boson mass of 115 GeV and for an integrated luminosity of 10 fb^{-1} , expected numbers of signal events (S), numbers of background events (B) and signal significances (S/\sqrt{B}) in ATLAS for the three dominant channels

	$H \rightarrow \gamma\gamma$	$t\bar{t}H \rightarrow t\bar{t}b\bar{b}$	$qqH \rightarrow qq\tau\tau \rightarrow \ell + X$
S	130	15	~ 10
B	4300	45	~ 10
S/\sqrt{B}	2.0	2.2	~ 2.7

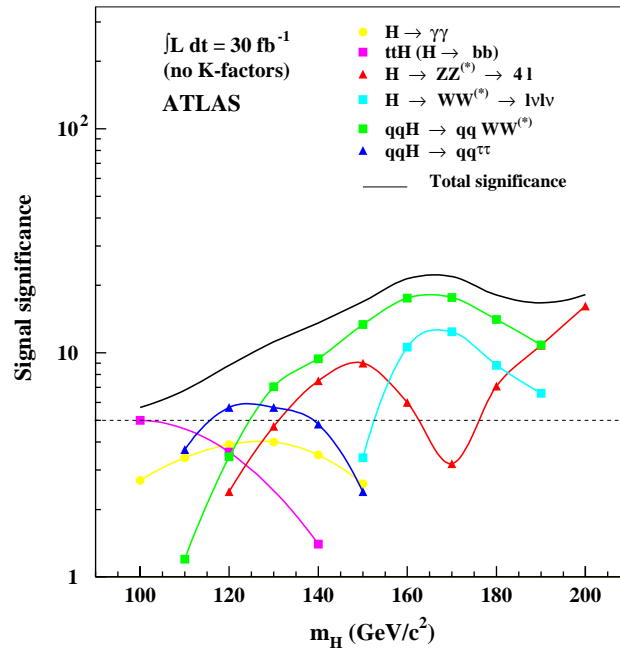


Fig. 6. The expected SM Higgs signal significance in ATLAS in the low-mass region for 30 fb^{-1} . The total significance (full line) and the contributions of the individual channels (symbols) are shown.

a convincing signal with only 10 fb^{-1} , because the significances of the individual channels are small, and because an excellent knowledge of the backgrounds and close-to-optimal detector performances are required, as discussed below. Therefore, the contribution of both experiments, and the observation of possibly all three channels, will be crucial for an early discovery.

We stress that the channels listed in Table 2 are complementary. Indeed, they are characterized by different production mechanisms and decay modes, and therefore by different backgrounds and different detector requirements:

- Excellent performance of the electromagnetic calorimeters is crucial for the $H \rightarrow \gamma\gamma$ channel, since a mass resolution of $\sim 1\%$ is needed to observe a narrow signal peak on top of the irreducible $\gamma\gamma$ background. This requires a calorimeter response uniformity of $\sim 0.5\%$ over the full rapidity coverage, which will be extremely challenging to achieve in the first year of operation.

- Efficient and powerful b -tagging is the crucial performance issue for the $t\bar{t}H$ channel, since there are four b -jets in the final state which all need to be tagged in order to reduce the background ($t\bar{t}jj$ production and combinatorial from the signal itself).
- Efficient and precise jet reconstruction over ten rapidity units ($|\eta| < 5$) is needed for the $H \rightarrow \tau\tau$ channel, since tagging of the two forward jets accompanying the Higgs boson and vetoing any additional jet activity in the central region of the detector are necessary tools to defeat the background (dominated by $Z + \text{jet}$ production with $Z \rightarrow \tau\tau$).

The above channels require a control of the backgrounds at the level of a few percent. This shall be achieved mainly by using the data (the best of all “simulations” ...), for instance by directly measuring the (smooth) $\gamma\gamma$ background rate in the side-bands of the $H \rightarrow \gamma\gamma$ signal region, or by using dedicated control samples (e.g. $t\bar{t}jj$ production, where the jets j are tagged as light-quark or gluon jets, provides a normalization for the irreducible $t\bar{t}b\bar{b}$ background to the $t\bar{t}H$ channel).

With more integrated luminosity than 10 fb^{-1} , the observation of the Higgs boson will become unambiguous even for low mass values, as depicted in Figs. 5 and 6. It should also be noticed that over most of the m_H range two or more decay channels will be detected, thus providing robustness to the discovery and additional hints to understand the nature of the signal.

In conclusion, after about 3 years of operation the LHC should provide the final word about the SM Higgs mechanism: if nothing were to be found, other mechanisms would have to be investigated.

These results are based not only on simulation studies, but also on test-beam measurements of detector modules. As an example, Fig. 7 shows the γ/π^0 separation capability of the ATLAS electromagnetic calorimeter, as obtained from beam tests of series production modules [21]. In order to suppress the γ -jet and jet-jet backgrounds to a possible $H \rightarrow \gamma\gamma$ signal, a rejection of ~ 3 against π^0 's faking single photons is needed. The test-beam results show that such a performance can be achieved, and that the data are well reproduced by the simulation.

If a Higgs boson were to be discovered at the LHC, ATLAS and CMS should be able to perform several precise measurements of its properties. For example, with the ultimate integrated luminosity of 300 fb^{-1} per experiment the Higgs mass should be measured with the remarkable experimental precision of 0.1% over the mass region up to $\sim 400 \text{ GeV}$. This direct measurement can then be compared to the indirect determination of m_H obtained from the measurements of the W and top masses. The expected precisions at the LHC are $\sim 15 \text{ MeV}$ on m_W and $\sim 1 \text{ GeV}$ on m_{top} [13], leading to a 25% (indirect) accuracy on the mass of a light Higgs boson. Such a comparison will provide crucial tests of the internal consistency of the theory, in particular of the electroweak symmetry breaking sector. As another example, ratios of Higgs couplings to fermions and bosons should be determined with typical precisions of 20% [22], as shown in Fig. 8. The Higgs self-coupling λ , which is of utmost importance since it gives access to the Higgs-field potential in the SM Lagrangian, is not accessible at the standard LHC, but might be measured with an interesting precision of $\sim 20\%$ [23] at an upgraded LHC operating at a luminosity $L = 10^{35} \text{ cm}^{-2} \text{ s}^{-1}$. Finally, several studies [24] indicate that the spin-zero nature of the Higgs particle can be determined in the mass region covered by the $H \rightarrow 4\ell$ channel from the angular distributions of the final-state leptons. These measurements, although they cannot compete with the precision expected at a sub-TeV Linear Collider [25], where e.g. the various couplings should be constrained to the percent level (except for the self-coupling), should nevertheless establish the nature of the observed particle and provide major insights into the electroweak symmetry breaking mechanism.

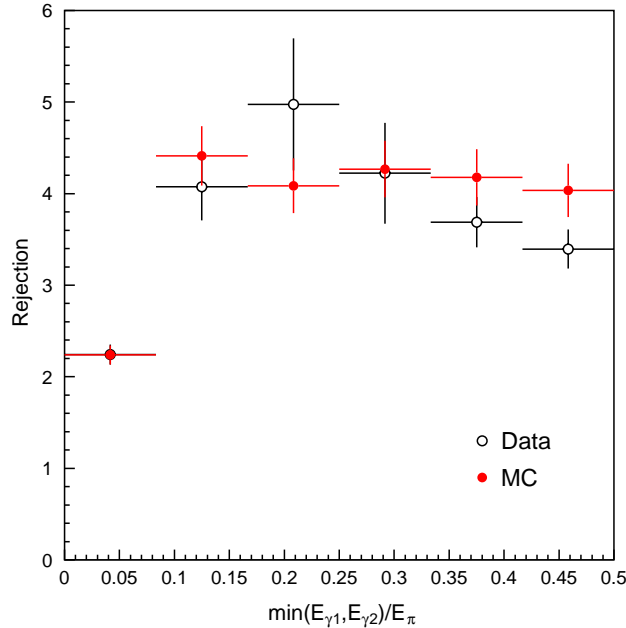


Fig. 7. Rejection against π^0 with $p_T \sim 50$ GeV, for a 90% efficiency for single photons, as a function of the energy fraction carried by the less energetic photon. The open symbols show results from test-beam data collected with final modules of the ATLAS liquid-argon electromagnetic calorimeter and a special photon beam, whereas the dots indicate the prediction of the Geant3 simulation.

5. Searches for Supersymmetry and beyond ...

Supersymmetry [26], a very attractive symmetry relating fermions and bosons, i.e. matter fields and force fields, is probably the best motivated scenario today for physics beyond the SM [4]. It does not contradict the precise, and therefore very constraining, electroweak data, it predicts a light Higgs boson, as favoured by these data, it allows unification of the gauge couplings at the Grand Unification scale and a natural incorporation of gravity, it is an essential element of string theories, it provides a candidate particle for the universe cold dark matter. In particular, it is able to stabilize the Higgs boson mass, through radiative corrections, provided that the SUSY particles (sparticles) have masses at the TeV scale or below. In spite of these numerous motivations, we have no experimental evidence for Supersymmetry as of today. Direct searches for sparticles at LEP and Tevatron have been unsuccessful, and have set mass lower bounds in the range 90–300 GeV depending on the sparticle type.

We recall that in Supersymmetry for each SM particle p there exists a supersymmetric partner \tilde{p} with identical quantum numbers except the spin which differs by half a unit. The sparticle spectrum predicted by minimal SUSY models, such as the Minimal Supersymmetric extension of the Standard Model (MSSM [26]), is given in Table 3.

Important phenomenological consequences arise from the fact that the theory contains a multiplicative quantum number, called R-parity, which takes opposite values for SM and SUSY particles. The conservation of R-parity, motivated by cosmological arguments, is assumed here. This implies that sparticles are produced in pairs and that the Lightest Supersymmetric Particle (LSP), to which all sparticles eventually

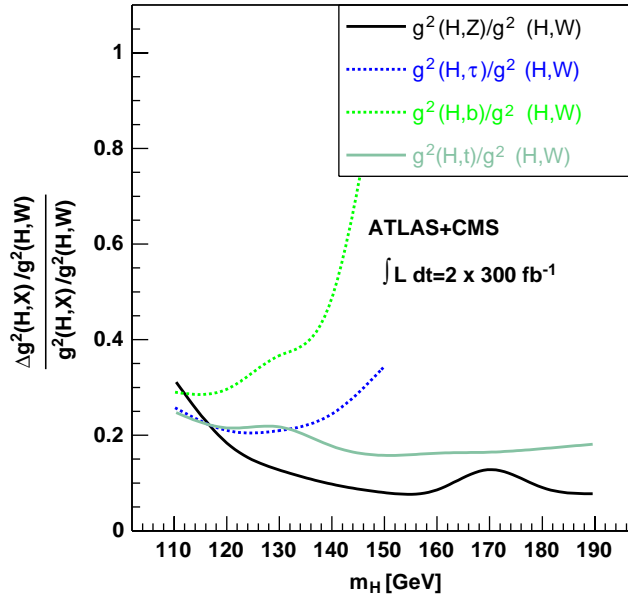


Fig. 8. The expected experimental precision on the measurements of ratios of Higgs couplings to fermions and bosons at the LHC, as a function of mass and for an integrated luminosity of 300 fb^{-1} per experiment. Systematic uncertainties are included.

Table 3
Standard Model particles and their supersymmetric partners in the MSSM

SM particles	SUSY partners	Spin of SUSY partners
Quarks	Squarks \tilde{q}	0
Leptons	Sleptons $\tilde{\ell}$	0
Gluon	Gluino \tilde{g}	1/2
W^\pm, H^\pm -field	Charginos $\chi_{1,2}^\pm$	1/2
Z, γ, H -field	Neutralinos $\chi_{1,2,3,4}^0$	1/2

decay, must be stable. In most models the LSP is the lightest neutralino χ_1^0 , which is a stable, massive and weakly interacting particle, and therefore an excellent candidate for the universe cold dark matter.

At the LHC, the dominant SUSY process is expected to be the production of pairs of squarks or gluinos, because these are strongly-interacting particles with QCD-type cross-sections. For instance, a sample of about 10^4 $\tilde{q}\tilde{q}, \tilde{g}\tilde{g}$ and $\tilde{q}\tilde{g}$ events should be produced over only 1 year of data taking at $L = 10^{33} \text{ cm}^{-2} \text{ s}^{-1}$ if squarks and gluinos have masses of $\sim 1 \text{ TeV}$. Because these sparticles weigh at least 200–300 GeV, given the present Tevatron limits, they are expected to decay through long chains with several intermediate steps, and hence should give rise to very busy final states containing in general several jets, leptons and missing transverse energy. The latter is due to the fact that, if R-parity is conserved, in each SUSY event two neutral and weakly interacting LSPs are produced, which escape experimental detection. Such spectacular signatures can be easily separated from SM processes, for instance by selecting events with many high- p_T jets and large missing transverse energy.

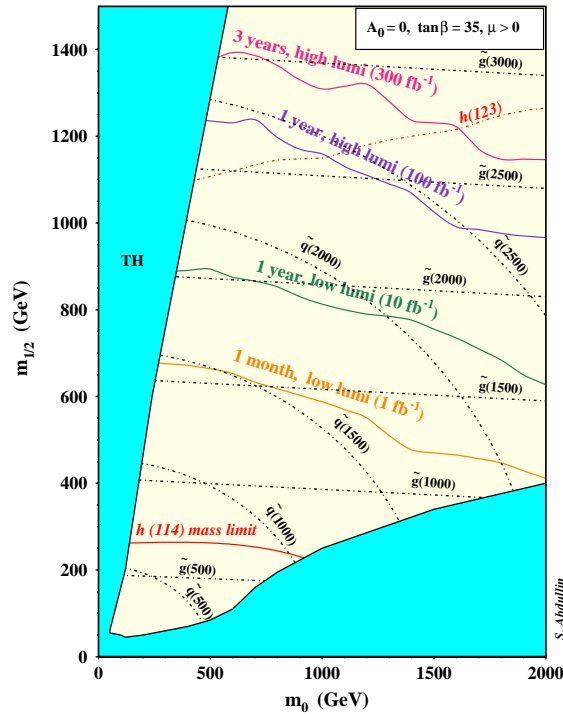


Fig. 9. The CMS discovery potential for squarks and gluinos as a function of integrated luminosity (full lines). Squark and gluino mass isolines (dot-dashed) are shown (masses are given in GeV). The universal scalar mass m_0 and the universal gaugino mass $m_{1/2}$ are two fundamental parameters of the theory.

As a consequence, SUSY discovery at the LHC could be relatively easy and fast, as shown in Fig. 9. Squark and gluino masses of 1 TeV are accessible after only one month of data taking at $L=10^{33} \text{ cm}^{-2} \text{ s}^{-1}$, once the backgrounds (e.g. $t\bar{t}$ production, mismeasured QCD multijet events) and the detector performance (in particular tails in the calorimeter response to jets) will have been well understood. The ultimate mass reach is up to ~ 3 TeV for squarks and gluinos. Therefore, if nothing is found at the LHC, TeV-scale Supersymmetry will most likely be ruled out, because of the arguments related to stabilizing the Higgs mass mentioned above.

On the other hand if SUSY is there, the LHC experiments should go beyond the mere discovery phase. They should be able to perform several precise measurements of the sparticle masses, and thus determine the fundamental parameters of the theory with a precision of $\sim 10\%$ or better in many cases, at least in minimal models like mSUGRA [27].

This capability, which has been demonstrated (within mSUGRA) for the first time in 1996, and represents one of the major breakthroughs in the understanding of the LHC physics potential, is based on the following technique. Since each event contains two escaping neutralinos, mass peaks for the produced sparticles cannot be reconstructed directly. However, the invariant mass distributions of the visible particles in the final state should exhibit threshold and end-point structures, which are related to the decay kinematics (and hence masses) of the sparticles produced at the various steps of the (long) squark and gluino decay chains.

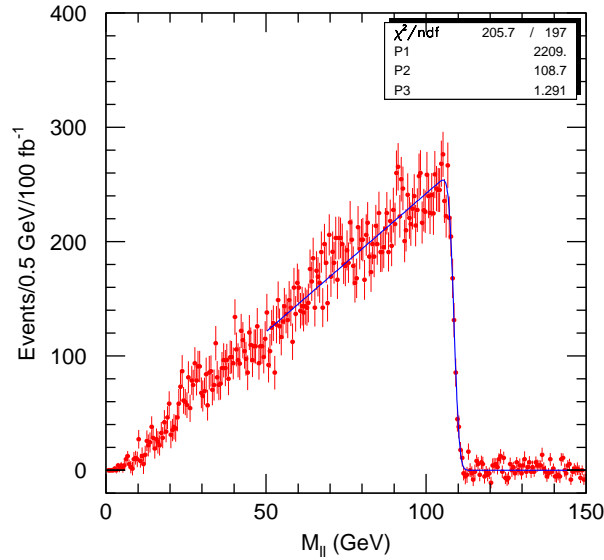


Fig. 10. Invariant mass distribution of e^+e^- and $\mu^+\mu^-$ pairs at “Point 5” of mSUGRA (see text), as obtained from an ATLAS simulation for an integrated luminosity of 100 fb^{-1} .

An example is depicted in Fig. 10 for a point in the mSUGRA parameter space (the so-called “LHC Point 5” [7]) which gives an amount of neutralino cold dark matter consistent with that predicted by inflation and where $m(\tilde{q}) \sim eq700\text{ GeV}$, $m(\tilde{g}) \sim eq800\text{ GeV}$, $m(\tilde{\ell}_R) = 160\text{ GeV}$, $m(\chi_2^0) \sim eq230\text{ GeV}$ and $m(\chi_1^0) \sim eq120\text{ GeV}$. A typical decay chain, not only at this point but over a large part of the parameter space, is $\tilde{q}_L \rightarrow q\chi_2^0 \rightarrow q\ell^+\ell^-\chi_1^0$. The invariant mass distribution for opposite-sign same-flavour lepton pairs in the final state, plotted in Fig. 10, shows a sharp end-point that is due to the two-body kinematics of the decay $\chi_2^0 \rightarrow \tilde{\ell}_R^*\ell \rightarrow \ell^+\ell^-\chi_1^0$. The position of this end-point, which can be measured with an experimental precision of a few permil in this region of the parameter space, is related to the masses of the involved sparticles (χ_2^0 , $\tilde{\ell}_R$, χ_1^0), and therefore provides a constraint on their combination. Similarly, $q\ell$ and $q\ell\ell$ invariant mass distributions yield constraints on the sparticle masses involved higher up in the decay chain. This reconstruction procedure is expected to be quite general, and applicable also to less-constrained models than mSUGRA, since over most of the SUSY parameter space one or more such (long) decay chains should be available. Threshold and end-point structures can be measured with experimental precisions as good as a few permil (if leptons are involved) and a few percent (if jets are involved), where the dominant systematic uncertainties are expected to come from the knowledge of the lepton and jet absolute energy scales. The ensemble of experimental measurements of this type shall provide a set of equations, which can be solved in terms of the (unknown) masses of the produced sparticles.

We anticipate that the correct identification of the underlying theory and the measurements of its fundamental parameters will not be easy for general models with many unknown parameters. It is however hoped that, by exploiting the expected richness of the data with a lot of different measurements (masses, cross-sections, decay modes, etc.) and observations (e.g. excess of events with b -quarks or taus), and with some guidance from theory, it will eventually be possible to narrow the a priori large spectrum of models and pin down the correct framework.

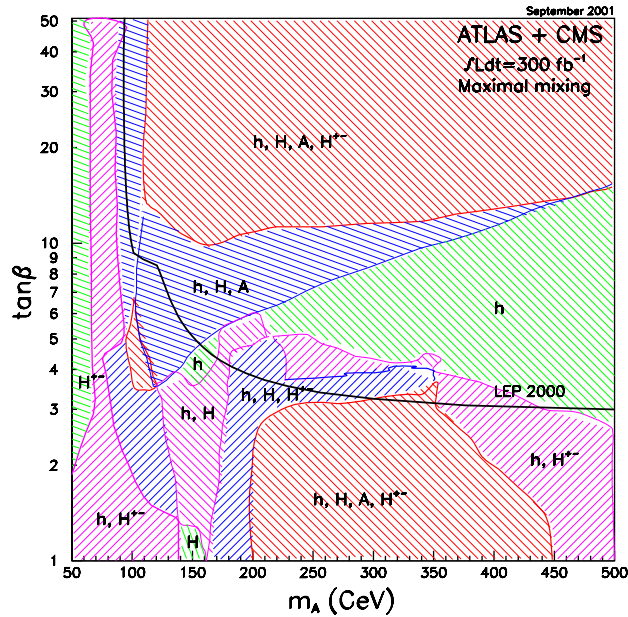


Fig. 11. The regions of the (constrained) MSSM plane $\{m_A - \tan \beta\}$ where the various Higgs bosons can be discovered at the LHC through their decays into SM particles. The region below the thick curve has been excluded by LEP.

We note also that, by using the method described above, it should be possible to determine indirectly the mass of the (invisible) lightest neutralino, the dark matter candidate, which would obviously have important cosmological implications. At Point 5 the expected experimental precision is about 10%. Furthermore, once the underlying SUSY model will have been identified, a fit of this model to the ensemble of experimental measurements should allow the density of the universe cold dark matter to be estimated, assuming the latter is composed only of relic neutralinos. A study performed within mSUGRA at Point 5 indicates an ultimate precision of about 2%. Similar precisions have been obtained in other regions of the parameter space [28]. Eventually, comparisons of these and other results to astroparticle measurements (like the recent observations of the WMAP satellite [29] or the future explorations by the Planck telescope [30]) and cosmological predictions should establish whether the features of the neutralinos observed at the LHC are compatible with this particle being the constituent of the universe cold dark matter. Such a result would be a major interdisciplinary achievement for the LHC and CERN.

A rich phenomenology is also expected from the SUSY Higgs sector, which consists of five bosons, three neutral (h, H, A) and two charged (H^\pm). The mass of the lightest one, h , is predicted to be below 135 GeV, whereas the others are expected to be heavier and essentially mass-degenerate over most of the parameter space.

The Higgs sector of the MSSM can be described in terms of the mass of the A boson m_A and of the parameter $\tan \beta$ (the ratio of the vacuum expectation values of the two Higgs doublets which give rise to the five physical states). Fig. 11 shows the regions of this parameter space where the various Higgs bosons can be discovered at the LHC through their decays into SM particles. The capability of detecting final states containing taus, arising, e.g. from $A/H \rightarrow \tau\tau$ or $H^\pm \rightarrow \tau^\pm \nu$ decays, is expected to be crucial to explore the SUSY Higgs sector at the LHC. It can be seen that over a large fraction of the

Table 4

Examples of the LHC ultimate discovery potential for some scenarios beyond the Standard Model

Scenario/channel	Reach
$Z' \rightarrow \ell\ell$	$m \sim 5 \text{ TeV}$
$W' \rightarrow \ell\nu$	$m \sim 6 \text{ TeV}$
Leptoquarks	$m \sim 1.5 \text{ TeV}$
Compositeness	Compositeness scale $\Lambda \sim 40 \text{ TeV}$
Excited quarks	$m \sim 6.5 \text{ TeV}$
Extra-dimensions	Gravity scale $M \sim 9 \text{ TeV}$ for 2 extra-dimensions
Monopoles	$m \sim 20 \text{ TeV}$

parameter space two or more Higgs bosons should be observed. The only exception is the region at large m_A and moderate $\tan\beta$, where only h can be discovered at the LHC, unless the heavier Higgs bosons have observable decays into SUSY particles. The LHC may therefore miss part of the SUSY Higgs spectrum. A direct observation of the complete spectrum would then have to wait for a multi-TeV lepton collider like CLIC [31].

Many other examples of physics beyond the Standard Model have been studied by the LHC experiments: theories with Extra-dimensions, Little Higgs models, Technicolour, Compositeness, etc. Since we do not know today which scenario Nature has chosen, the aim of these studies was to verify that ATLAS and CMS will not miss any relevant expected topology (in particular at the trigger level) and that they are able to address as many signatures as possible. It is particularly encouraging to note that some signatures which were not well known in the experimental LHC community in the early 1990s when the detectors were designed (e.g. the non-pointing photons and the heavy stable charged particles predicted by Gauge-Mediated-SUSY-Breaking models [32]) turned out later on to be accessible with good efficiency, which demonstrates the robustness of ATLAS and CMS and their potential capability to cope with the unexpected.

The LHC discovery potential for some scenarios beyond the SM is illustrated in Table 4. In most cases the direct reach extends well beyond the 1 TeV “threshold”. More details can be found in Refs. [7,8,33].

6. Studies of quark–gluon plasma

The LHC will also be able to collide beams of nuclei, thereby providing ultra-relativistic heavy-ion interactions at an energy of 5.5 TeV per nucleon, i.e. a total centre-of-mass energy of more than 1000 TeV in the case of lead beams. These collisions will allow the study of strongly interacting matter in unprecedented and extreme conditions of energy density and temperature. In these conditions, a phase transition from ordinary hadronic matter to a plasma of deconfined quarks and gluons is expected to happen. Because the opposite transition (i.e. from plasma to hadronic matter) is believed to have taken place about 10 μs after the Big Bang (i.e. when the universe temperature was $T \sim eq\Lambda_{\text{QCD}} \sim eq200 \text{ MeV}$), these studies should also provide clues to understand the evolution of the early universe. In addition, they should address the fundamental questions of quark confinement and approximate chiral-symmetry restoration. It should be noted that QCD phase transition is the only transition of elementary fields accessible in a laboratory. Heavy-ion collisions will therefore open a different territory from that explored by ATLAS, CMS and LHCb, thereby offering a significant and exciting enhancement to the overall LHC physics potential.

Table 5

Main features of ultra-relativistic heavy-ion collisions at the SPS, RHIC and LHC

	SPS	RHIC	LHC
Colliding ions	Pb–Pb	Au–Au	Pb–Pb
Centre-of-mass energy per nucleon pair (GeV)	17	200	5500
Energy density (GeV/fm ³)	~ 3	~ 5	15–60
Freeze-out volume (fm ³)	~ 10 ³	~ 7 × 10 ³	~ 20 × 10 ³
QGP lifetime (fm/c)	≤ 1	1.5–4	≥ 10
Number of charged particles per rapidity unit	400	800	~ 3000

Although several hints for the production of a quark–gluon plasma (QGP) in ultra-relativistic heavy-ion collisions exist from the CERN SPS [34] and the RHIC collider at BNL [35], unambiguous experimental evidence is still lacking, and a consistent theoretical scenario of the phase transition and related manifestations has not emerged from the available data yet.

At the LHC, thanks to the very high temperature of the collisions, deconfinement and QGP formation are expected to become routine phenomena. As illustrated in Table 5, which lists some features of ultra-relativistic nucleus–nucleus interactions at various machines, the energy density, the volume of the collision region and the QGP lifetime should all increase by large factors at the LHC compared to the SPS and RHIC (although there are large uncertainties in the predictions). This will hopefully allow powerful, detailed and comprehensive studies of the phase diagram for nuclear matter.

Among the most relevant and experimentally accessible probes of QGP formation, the suppression of J/ψ and Υ states is expected, because colour-screening effects in the hot dense medium can prevent quark–antiquark pairs from combining. In addition, since the different quarkonia states have different binding energies, and therefore different dissociation temperatures, some of them will be suppressed and some others will not, depending on the critical temperature at which the phase transition occurs. Therefore these resonances may act as QCD thermometers for the quark–gluon plasma.

Jet quenching, i.e. energy losses by partons (through gluon radiation) while traversing the plasma, will lead to anomalous features in the production of jets and hadrons as compared to pp interactions. First evidence for such phenomena has been recently reported by the RHIC experiments [36], which have observed a suppression of high- p_T single-hadron yields in Au–Au collisions as compared to pp collisions.

Prompt photons are expected to be emitted, e.g. by thermal radiation from the plasma, and their p_T spectrum should be sensitive to different stages of the system evolution (pre-equilibrium, thermalization, etc.). Finally, the p_T spectra and the ratios of production rates for different hadron species, as a function of the particle density, probe the thermalization phase and the dynamic evolution of the hadronic phase.

The price to pay for the increased physics potential is that the experimental environment will also in this case be much more challenging at the LHC than at previous machines. Table 5 shows that a few thousand charged particles are expected to be produced per rapidity unit at each Pb–Pb interaction, which imposes stringent requirements on the detector design and performance. Heavy-ion collisions at the LHC will be studied to a certain extent by ATLAS and CMS, but much more in detail by the dedicated ALICE experiment, which has been conceived to cope with a very high-multiplicity environment and to detect the above and other signatures of QGP formation. Since different probes may be sensitive to different stages of the evolution from nuclear matter to QGP and back to ordinary matter, and since there exists as yet no

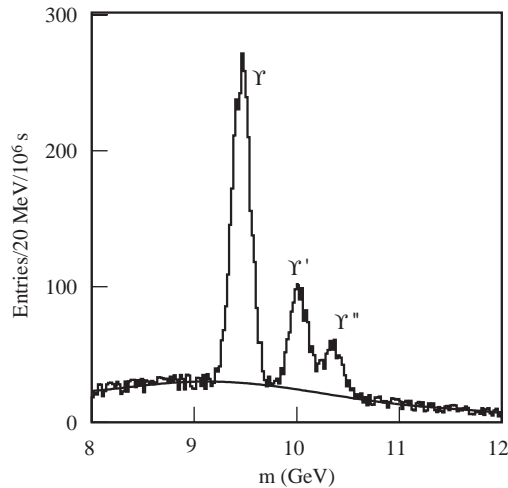


Fig. 12. Di-muon invariant mass distribution expected in ALICE after about one month of data taking, showing the resonances of the Υ family on top of the background.

complete picture of the phenomena occurring at the phase transition, ALICE is a multi-purpose experiment [6,10] able to detect as many topologies as possible. As an illustration of the expected performance, Fig. 12 shows a simulation of Υ resonances in the di-muon decay channel on top of the background. A clear separation between Υ , Υ' and Υ'' is visible, which is important since observation (or lack thereof) of some of these states will provide constraints on the critical temperature of the system.

7. Conclusions

In about 3 years from now the LHC will start operation, and CERN and experimental particle physics will enter a new epoch, hopefully the most glorious and fruitful of their history.

Given the compelling motivations for new physics at the TeV scale, one can anticipate a profusion of exciting (and perhaps unexpected ... ?) results from a machine able to explore this scale in detail, with a direct discovery potential up to particle masses of $\sim 5\text{--}6$ TeV. As a consequence, the LHC should provide definitive answers about the SM Higgs mechanism, Supersymmetry, and several other TeV-scale predictions that have resisted experimental verification for decades.

In addition, the LHC experiments will be able to make many precise measurements of known and possibly new particles, and will shed additional light on the mystery of CP-violation; they will perform several studies in an energy regime overlapping with the high-energy part of the cosmic ray spectrum; they will probe in detail the properties of the quark–gluon plasma, the bulk of matter filling the universe a few microseconds after the Big Bang.

These goals are possible thanks to a machine and detectors of unprecedented performance and complexity. In particular, the sensitivity of the experiments to a huge number of signatures, topologies and models has been demonstrated in great detail over 15 years of simulation efforts and test-beam measurements, and this provides great faith in their robustness and potential ability to cope also with unexpected scenarios.

Today, about 3 years before the beginning of data taking, we can hope that the LHC will add many crucial pieces to our knowledge of fundamental physics, and will therefore also have a big impact on astrophysics and cosmology. More importantly, perhaps, we can hope that it will tell us which are the right questions to ask.

Acknowledgements

I would like to thank Kevin Einsweiler, Daniel Fournier, Daniel Froidevaux, Peter Jenni, Gigi Rolandi and Frederic Teubert for their useful comments.

References

- [1] G. Altarelli, M.W. Grünewald, *Phys. Rep.* (2004), this volume [doi:10.1016/j.physrep.2004.08.013].
- [2] Y. Fukuda, et al., *Phys. Rev. Lett.* B 81 (1998) 1562.
- [3] Q.R. Ahmad, et al., *Phys. Rev. Lett.* 87 (2001) 071301.
- [4] J. Ellis, M. Jacob, *Phys. Rep.* (2004), this volume [doi:10.1016/j.physrep.2004.08.015].
- [5] D. Treille, Searches for new particles at LEP, this issue.
- [6] ALICE Collaboration, Technical Proposal, CERN/LHCC 95-71.
- [7] ATLAS Collaboration, Detector and Physics Performance Technical Design Report, CERN/LHCC/99-15, 1999.
- [8] CMS Collaboration, The Compact Muon Solenoid, Technical Proposal, CERN/LHCC/94-38, 1994; see also <http://cmsdoc.cern.ch/cms/PRS/results>.
- [9] LHCb Collaboration, Technical Proposal, CERN/LHCC/98-004; LHCb Collaboration, Reoptimized Detector Technical Design Report, CERN/LHCC/2003-030.
- [10] T.S. Virdee, *Phys. Rep.* (2004), this volume [doi:10.1016/j.physrep.2004.08.026].
- [11] G. Brianti, *Phys. Rep.* (2004), this volume [doi:10.1016/j.physrep.2004.08.029].
- [12] Large Hadron Collider in the LEP tunnel, Proceedings of the ECFA–CERN Workshop, ECFA 84/85, CERN 84-10.
- [13] G. Altarelli, M. Mangano (Eds.), Proceedings of the Workshop on Standard Model Physics (and more) at the LHC, CERN 2000-004.
- [14] J. Christenson, et al., *Phys. Rev. Lett.* 13 (1964) 138.
- [15] H. Wahl, *Phys. Rep.* (2004), this volume [doi:10.1016/j.physrep.2004.08.007]; J.R. Batley, et al., *Phys. Lett.* B 544 (2002) 97.
- [16] R. Forty, *Phys. Rep.* (2004), this volume [doi:10.1016/j.physrep.2004.08.016].
- [17] B. Aubert, et al., *Phys. Rev. Lett.* 86 (2001) 2515.
- [18] K. Abe, et al., *Phys. Rev. Lett.* 87 (2001) 091802.
- [19] ALEPH, DELPHI, L3 and OPAL Collaborations, *Phys. Lett.* B 565 (2003) 61.
- [20] CDF and D0 Collaborations, Results of the Tevatron Higgs sensitivity study, FERMILAB-PUB-03/320-E, October 2003.
- [21] ATLAS Electromagnetic Liquid Argon Calorimeter group, Performance of the fine lateral segmentation of the first compartment of the ATLAS EM calorimeter, *Nucl. Instrum. Methods*, submitted for publication.
- [22] M. Dührssen, ATLAS Note ATL-PHYS-2003-030.
- [23] U. Baur, T. Plehn, D. Rainwater, *Phys. Rev.* D 67 (2003) 033003.
- [24] See for instance C.P. Buszello, et al., *Eur. Phys. J.* C 32 (2003) 209.
- [25] TESLA Technical Design Report, hep-ph/0106315.
- [26] For a phenomenological review see for instance P. Fayet, S. Ferrara, *Phys. Rep.* C 32 (1977) 249; H.P. Nilles, *Phys. Rep.* C 110 (1984); H.E. Haber, G.L. Kane, *Phys. Rep.* C 117 (1985) 75.
- [27] A.H. Chamseddine, R. Arnowitt, P. Nath, *Phys. Rev. Lett.* 49 (1982) 970.
- [28] G. Polesello, D. Tovey, ATLAS Note ATL-PHYS-2004-008.

- [29] C.L. Bennet, et al., *Astrophys. J. Suppl.* 148 (2003) ;
D.N. Spergel, et al., *Astrophys. J. Suppl.* 148 (2003) 175;
H.V. Peiris, et al., *Astrophys. J. (Suppl.)* 148 (2003) 213.
- [30] J.A. Tauber, The Planck mission, in: *Proceedings of Symposium no. 201 of the International Astronomical Union, Manchester, August 2000.*
- [31] I. Wilson, *Phys. Rep.* (2004), this volume [doi:10.1016/j.physrep.2004.08.028].
- [32] G.F. Giudice, R. Rattazzi, *Phys. Rep.* 322 (1999) 419;
S. Ambrosiano, G.D. Kribs, S.P. Martin, *Phys. Rev. D* 56 (1997) 1761.
- [33] B.C. Allanach, et al., *Les Houches Physics at TeV Colliders 2003: Beyond the Standard Model Working Group Summary Report*, hep-ph/0402295.
- [34] H. Satz, *Phys. Rep.* (2004), this volume [doi:10.1016/j.physrep.2004.08.009].
- [35] See for instance M. Lisa, *What have we learned so far? An experimental perspective*, talk given at Quark Matter 2004, Oakland, January 2004, <http://www.lbl.gov/nsd/qm2004/program.html>.
- [36] B.B. Back, et al., *Phys. Rev. Lett.* 91 (2003) 072302;
S.S. Adler, et al., *Phys. Rev. Lett.* 91 (2003) 072303;
I. Arsene, et al., *Phys. Rev. Lett.* 91 (2003) 072305;
J. Adams, et al., *Phys. Rev. Lett.* 91 (2003) 072304.